Quaternary Research 71 (2009) 375–384

Contents lists available at ScienceDirect

Quaternary Research

journal homepage: www.elsevier.com/locate/yqres

North Atlantic control on precipitation pattern in the eastern Mediterranean/Black Sea region during the last glacial

Olga Kwiecien [a,b,*], Helge W. Arz [a], Frank Lamy [c], Birgit Plessen [a], André Bahr [d], Gerald H. Haug [b,e]

[a] Helmholz Centre Potsdam, GFZ German Research Centre for Geosciences, 14473 Potsdam, Germany
[b] DFG-Leibniz Center for Surface Process and Climate Studies at Universität Potsdam, Germany
[c] Alfred Wegener Institute for Polar and Marine Research (AWI), 27570 Bremerhaven, Germany
[d] IFM-GEOMAR, 24148 Kiel, Germany
[e] Swiss Federal Institute of Technology (ETH Zürich), CH-8092 Zürich, Switzerland

ARTICLE INFO

Article history:
Received 30 November 2007
Available online 30 January 2009

Keywords:
Black Sea
Mediterranean
Paleoclimate
Precipitation
Terrigenous input
Heinrich events

ABSTRACT

Based on proxy records from western Black Sea cores, we provide a comprehensive study of climate change during the last glacial maximum and late-glacial period in the Black Sea region. For the first time we present a record of relative changes in precipitation for NW Anatolia based on variations in the terrigenous supply expressed as detrital carbonate concentration. The good correspondence between reconstructed rainfall intensity in NW Anatolia and past western Mediterranean sea surface temperatures (SSTs) implies that during the glacial period the precipitation variability was controlled, like today, by Mediterranean cyclonic disturbances. Periods of reduced precipitation correlate well with low SSTs in the Mediterranean related to Heinrich events H1 and H2. Stable oxygen isotopes and lithological and mineralogical data point to a significant modification in the dominant freshwater/sediment source concomitant to the meltwater inflow after 16.4 cal ka BP. This change implies intensification of the northern sediment source and, with other records from the Mediterranean region, consistently suggests a reorganization of the atmospheric circulation pattern affecting the hydrology of the European continent. The early deglacial northward retreat of both atmospheric and oceanic polar fronts was responsible for the warming in the Mediterranean region, leading simultaneously to more humid conditions in central and northern Europe.

Introduction

Recent studies on glacial millennial-scale climate variability carried out in the Mediterranean Sea have demonstrated that this region reacted very sensitively to rapid climatic and oceanographic changes in the North Atlantic realm related to the well-known Heinrich events (HEs) (e.g., Bond et al., 1993). The response to these cooling events was identified in both marine (Cacho et al., 1999, 2001, 2006; Sierro et al., 2005) and terrestrial (Allen et al., 1999; Combourieu Nebout et al., 2002; Sánchez Goñi et al., 2002) records from the western and central Mediterranean region in a variety of proxies. For the last glacial maximum (LGM) and late-glacial period, terrestrial and marine Mediterranean archives with reliable chronological control draw a similar picture: a generally positive hydrological balance marked by pronounced dry spells corresponding to HEs.

Western Mediterranean marine records show decreased sea surface temperatures (Cacho et al., 1999), decreased deep-water temperatures and intensified ventilation (Cacho et al., 2006) corresponding to HEs. Pollen data from the western and central Mediterranean document that arid and cold conditions over western Europe were synchronous to the response of the marine domain to the HEs (Allen et al., 1999; Combourieu Nebout et al., 2002; Sánchez Goñi et al., 2002). There is a lack of glacial marine records from the eastern Mediterranean but ample evidence from terrestrial archives like Lake Lisan (Bartov et al., 2003; Prasad et al., 2004) indicate humid conditions punctuated by enhanced aridity linked to the North Atlantic coolings. Oscillations in the North Atlantic polar front and atmospheric Polar Front were suggested to transmit the high-latitude signals to mid-latitudes (Cacho et al., 2001). The generally positive glacial hydrological balance reconstructed for the Mediterranean region is in agreement with a postulated more southerly position of the jet stream and the associated westerlies during this time window (Prentice et al., 1992). A southward-shifted jet stream would lead to relatively wet conditions in southern Europe and the Mediterranean, and relatively arid conditions in northern and central Europe. Similarly, a northward retreat of the polar fronts could explain early deglacial changes in the European hydrological cycle. These opposing trends in precipitation across the European continent during the LGM and late-glacial could be best observed in the differences in north European and Mediterranean lake status record (Harrison et al., 1996).

* Corresponding author. GeoForschungsZentrum Potsdam, 14473 Potsdam, Germany. Fax: +49 331 288 1302.
E-mail address: kwiecien@gfz-potsdam.de (O. Kwiecien).

0033-5894/$ – see front matter © 2009 University of Washington. All rights reserved.
doi:10.1016/j.yqres.2008.12.004

Published reconstructions of precipitation changes for the eastern Mediterranean region are either not long enough or of lower resolution. For example, two quantitative approaches using stable oxygen isotopes, a stalagmite record from Israel (Bar-Matthews et al., 1997) and an authigenic carbonate record from a crater lake in central Anatolia (Jones et al., 2007), propose very similar precipitation changes over the last glacial but these records do not reveal sufficient temporal resolution in the Marine Isotope Stage 2 (MIS 2) to distinguish the LGM from Heinrich Event 1 (H1). Pollen-based reconstruction (e.g., Mudie et al., 2002, 2007 and references therein) have alike suboptimal age control in MIS 2. Higher resolution reconstructions based on tree rings do not reach more that 900 yr ago (e.g., Touchan et al., 2007).

Here we introduce a record of precipitation changes in western Anatolia over the last 25 cal ka BP, based on variability of the terrigenous supply. We analyze changes in the composition of the terrigenous sediment fraction in order to identify modifications in the sediment input sources related to rainfall changes. To our advantage, the southern drainage area of the Black Sea (western Anatolia) is presently characterized by a Mediterranean-type climate while the northern drainage is under the influence of central European and north European climate. Tracing down the changes in composition of the terrigenous fraction provides a basis to reconstruct the relative contribution from these two regions and to understand interactions between the Mediterranean and central and north European hydrological regimes in the past. Finally, we present a close comparison between our Black Sea precipitation/sediment source record and other Mediterranean records, documenting major shifts in past atmospheric circulation patterns occurring concomitant to North Atlantic climate changes.

The last glacial Black Sea history

As the most distant arm of the Atlantic Ocean, the Black Sea demonstrates an unparalleled feature: it oscillates between lacustrine and marine stages following, respectively, glacial–interglacial sea level changes (Schrader, 1979). Today, the Black Sea is the world's largest anoxic basin. Therefore, most of the previous investigations have focused on its modern marine history covering the last ~8 ka. Only recent studies shed light on the glacial history of the western Black Sea (Major et al., 2002; Bahr et al., 2005) and the evolution of the hydrological properties of the basin during the last ~30 ka (Mudie et al., 2002; Bahr et al., 2006; Major et al., 2006).

During the glacial period, sedimentation in the Black Sea was dominated by terrigenous supply of siliciclastic material (Müller and Stoffers, 1974). Stable isotopes (Bahr et al., 2006) and Mg/Ca and Sr/Ca data (Bahr et al., 2008) measured on ostracods all point to relatively stable hydrological conditions of the Black Sea over this time interval. A series of reddish-brown clays occur in the sediments of the northern (Major et al., 2002; Ryan et al., 2003; Bahr et al., 2005) and the southern (Kwiecien et al., 2008) Black Sea after 16.4 cal ka BP. The intermission of the reddish-brown clays, commonly called 'red layers interval', was previously thought to represent meltwater pulses brought to the Black Sea by a Caspian spillover at the onset of the deglaciation (Bahr et al., 2005). This interpretation was supported by the similarity of the Black Sea red layers to the 'chocolate' clays representing glacial high stand of the Caspian Sea (Kroonenberg et al., 1997). Anomalies in the $\delta^{18}O$ signal (Bahr et al., 2006) and $^{87}Sr/^{86}Sr$ ratio (Major et al., 2006) of ostracod shells emphasized the significance of the melt/freshwater pulses on the Black Sea hydrology. As discussed in this paper, however, there

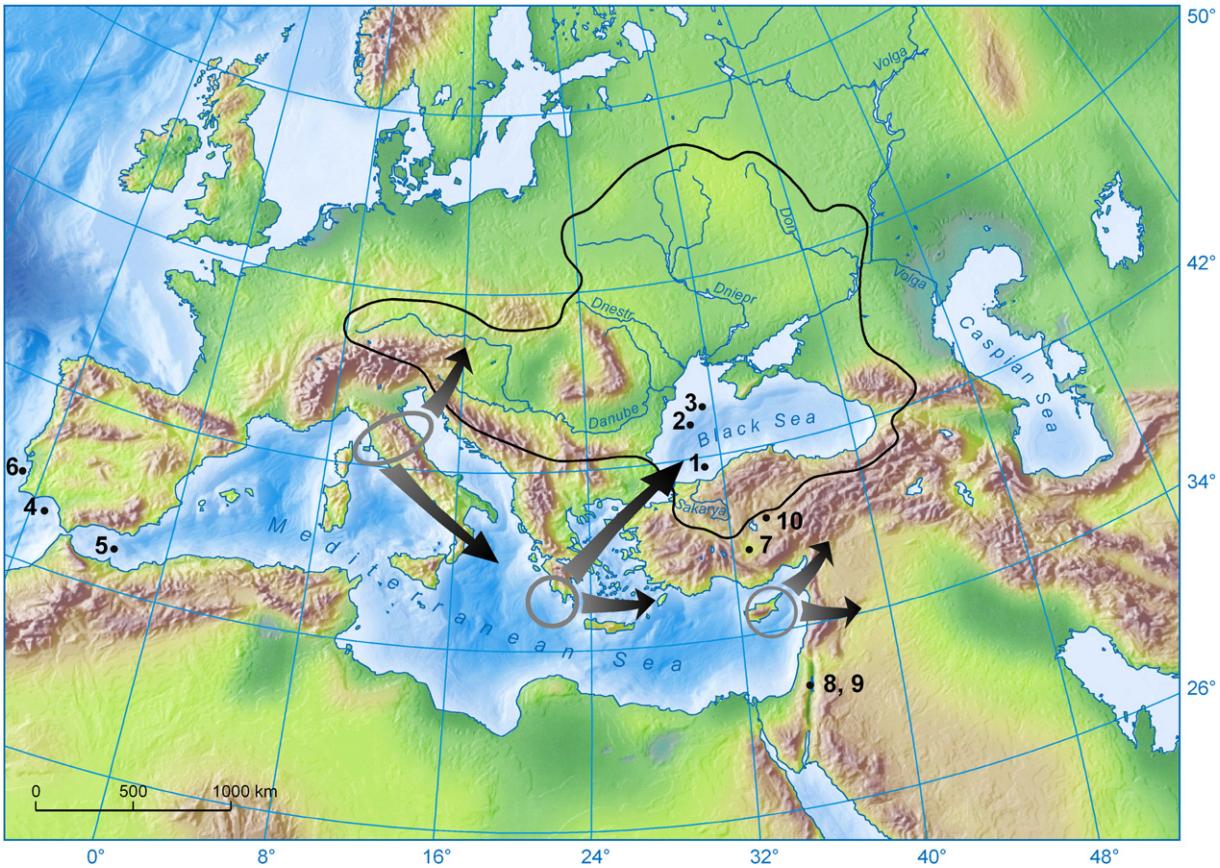

Figure 1. Regions of cyclogenesis (Mediterranean low-pressure systems) and principal cyclone tracks (based on Wigley and Farmer, 1982) together with locations of the sites relevant for the study. 1) MD04-2788/2760 this study; 2) GeoB 7608-1 (Bahr et al., 2006); 3) BLKS9809/10 (Major et al., 2002); 4) M39-008 (Cacho et al., 2000); 5) MD95-2043 (Cacho et al., 2000); 6) SU8118 (Bard et al., 2000); 7) Konya Plain lakes (Fontugne et al., 1999 and references therein); 8) Lake Lisan (Bartov et al., 2003); 9) Soreq Cave (Bar-Matthews et al., 1997); 10) Eski Acigöl (Jones et al., 2007). The black line indicates the area draining into the Black Sea.

https://doi.org/10.1016/j.yqres.2008.12.004 Published online by Cambridge University Press

are new findings that question the delivery of the red clays via the Caspian spillover. The Bølling/Allerød warming, which followed the deposition of the red layers, is recorded in the Black Sea sediments by a high amount of inorganically-precipitated carbonates (Major et al., 2002; Bahr et al., 2005). The inorganic carbonate precipitation was attributed to increased CO_2 assimilation due to massive phytoplankton blooms (Bahr et al., 2005). The carbonate precipitation, interrupted by the Younger Dryas cold interval, restarted in the early Holocene and continued until the reconnection with the Mediterranean Sea. The base of the Black Sea sapropel, traditionally marking the lacustrine/marine transition, is dated to ~8.0 cal ka BP (Lamy et al., 2006) but the first inflow of the Mediterranean water could have taken place as early as 9.5 cal ka BP (Bahr et al., 2006, 2008; Major et al., 2006).

Climatological and geological setting

Site MD04-2788/2760 is located at the continental slope of the southwestern coast of the Black Sea (NW Anatolia) off the mouth of the Sakarya River (Fig. 1). Today this region is influenced mainly by Mediterranean moisture sources and receives most of its rainfall during the winter/spring season. The rainfall in the eastern Mediterranean is primarily of cyclonic origin (Wigley and Farmer, 1982; Kostopoulou and Jones, 2007) (Fig. 1). Mediterranean SSTs play the key role in cyclogenesis; storms are formed along temperature gradient boundaries and are normally fed by moisture uptake from the relatively warm Mediterranean surface waters. Cyclones are more frequent and more intense during winter, when the atmosphere–sea-surface thermal gradient (difference between the temperature of the air aloft and the sea surface) is steepest. Consequently, the sediment load of the Sakarya and other Anatolian rivers, which follow the regional precipitation pattern, shows a strong seasonal component (Algan et al., 1999) (Fig. 2a).

The major part of the Sakarya River catchment (the upper river course composed of clastic continental rocks) is located in the Central Anatolia Plateau characterized by a dry to semi-dry climate (Fig. 2b). In contrary, a carbonate-bearing rocks domain is situated in the costal mountain area (lower river course) (Fig. 2b). The orographic effect causes a steep gradient between the rainfall amount received by the lower and by the upper course of the Sakarya River (Fig. 2b). The contribution of the lower course of the Sakarya River, receiving more rainfall over the year, is therefore more sensitive to changes in precipitation.

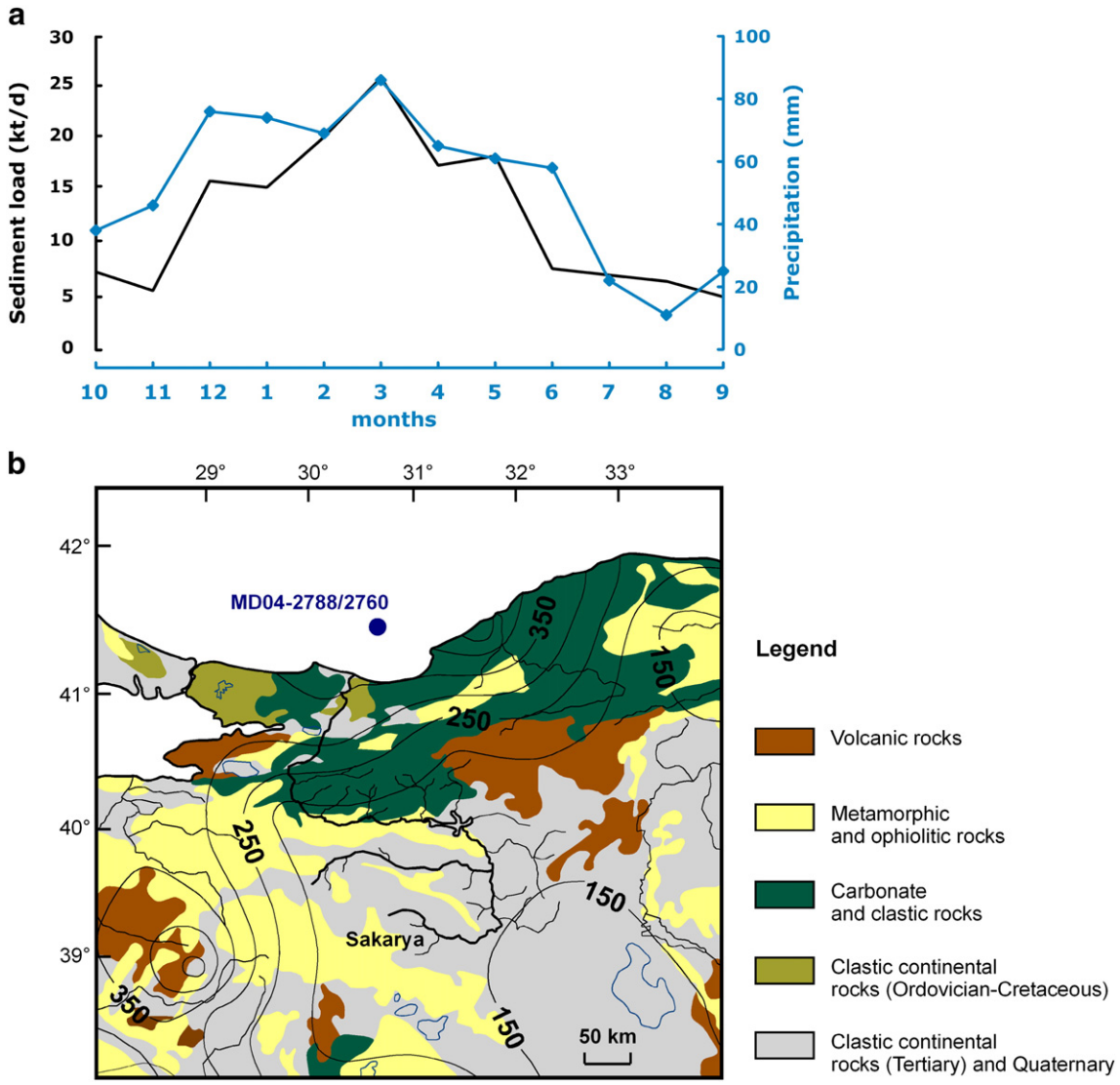

Figure 2. a: Relation of sediment load transported by Sakarya River to the amount of regional precipitation (Algan et al., 1999; the data were provided by the State General Directory of Electrical Research Works data base (EIE, 1993)). b: The distribution pattern of long-term average winter precipitation (mm) (after Türkes and Erlat, 2005) superimposed on a simplified geological map of NW Anatolia (modified after Geological Research Department of the General Directorate of Mineral Research and Exploration, 2002).

https://doi.org/10.1016/j.yqres.2008.12.004 Published online by Cambridge University Press

Material and methods

Material

The investigated record is a composite profile of the two sediment cores: MD04-2788 (gravity core for marine units) and MD04-2760 (piston core for lacustrine unit) (Kwiecien et al., 2008). Both cores were recovered from offshore northern Anatolia (Black Sea, 41°31.67′ N; 30°53.09′E) at a water depth of 1200 m (Fig. 1) during the ASSEMBLAGE I cruise of the R/V *Marion Dufresne*. The proximity of the Sakarya River results in very high sedimentation rates at the study site. The glacial section, with a sedimentation rate ranging from 1.5 m/ka to 2.5 m/ka, is continuously laminated and shows 1 to 5 mm-scale alternations of light-colored clay to darker-colored clay/fine silt (or sporadically fine sand). The period between 16.4 and 15 cal ka BP is marked by a prominent intercalation of reddish-brown fine clay material. Starting at the Bølling/Allerød and continuing until the early Holocene, biologically triggered precipitation of inorganic carbonates suppresses the terrigenous signal. Therefore the younger part of our record (14–8 cal ka BP) was discarded for the purpose of this study.

Profiling measurements

After splitting, cores MD04-2788 and MD04-2760 were scanned at 1-cm resolution with an AVAATECH X-ray fluorescence scanner at the University of Bremen, Germany. The XRF core scanner, developed at the Netherlands Institute for Sea Research, Texel, measures the bulk intensities of major elements (e.g., Al, Si, S, K, Ca, Ti, Mn, and Fe) on split sediment cores (Jansen et al., 1998).

$CaCO_3$ content

Samples were measured with an elemental analyzer (NC2500 Carlo Erba) at the GFZ Potsdam, Germany. Before the analysis the samples were freeze-dried and then ground and homogenized in an agate ball mill. Total carbon (TC) and total organic carbon (TOC) contents were determined in two separate runs. In the sediment samples for the organic carbon, the carbonate fraction was removed by addition of a 20% HCl solution. Sample duplicates show a reproducibility of 0.2%. TC and TOC were measured every 8 cm resulting in an average time resolution of ~40 yr. Starting at the first occurrence of the red layers (16.4 cal ka BP), the sampling resolution was increased to 4 cm, giving a time resolution of ~16 yr. Overall, 439 samples were analyzed. In order to calculate dry weight percentages of calcium carbonate ($CaCO_3$) we used the relation: $CaCO_3 = (TC - TOC) \times 8.33$.

Stable isotopes

Stable isotope analysis ($\delta^{18}O$) was performed on ostracod valves belonging to the genus *Candona* spp. (*C. schweyeri* and *C. angulata*). Either 5–8 valves of juvenile ostracods or 1–2 valves of adult ostracods were hand-picked from wet-sieved samples and analyzed at the University of Bremen using a Finnigan MAT 251 mass spectrometer with an automated carbonate preparation device. The ratio of $^{18}O/^{16}O$ is given in ‰ relative to the VPDB standard. Analytical long-time standard deviation is about ±0.07‰ VPDB. For the stable isotopes analysis we sampled the core MD04-2760 with U-channels integrating 4 cm in one sample (564 samples, 8 ml volume each). 135 samples did not provide enough ostracod shells for the measurement.

Chronology

Previous attempts to constrain a reliable chronology for lacustrine sediments were hampered by unknown reservoir age of the Black Sea water during its lacustrine stage. This obstacle is best depicted by significant differences in age models of two previously published records (Major et al., 2002; Bahr et al., 2005).

Presently, MD04-2788/2760 is the best-dated Black Sea record available for the LGM and Termination I, going back to ~25 cal ka BP. The chronological framework for the period of this study is based on calibrated AMS ^{14}C ages corrected for the reservoir effect, and on a clearly identified tephra layer (Table 1) (Kwiecien et al., 2008). The discovery of the Y-2 tephra, for the first time in the Black Sea sediments, turned out to be essential for the estimation of the reservoir effect during the glacial. Subsequent comparison of the calibrated MD04-2760 record with the Greenland ice core (GISP2) chronology (Grootes et al., 1993) suggests that the glacial reservoir age of 1450 ^{14}C yr decreased to 900 ^{14}C yr before the onset of the Bølling. The detailed examination of the XRF Ca-intensity signal allowed a precise correlation of the MD04-2788/2760 record with previously

Table 1
Details on age-control points used to construct age model for the composite profile MD04-2788/2760 (Kwiecien et al., 2008)

Sample	Original depth in the core (cm)	Depth in the composite profile (cm) MD04-2788/2760	^{14}C age (yr BP)	Applied reservoir correction	Calibrated age[a] (yr BP) ± 1σ	Material/source
Core MD04-2788						
KIA 28419	463–470	674–684	13,220 ± 70	900[b]	14,069–14,408	Ostracods
Core MD04-2760						
KIA 26701	945–965	643–663	13,050 ± 70	900[b]	13,919–14,094	Gastropod
KIA 25676	1540–1560	1238–1258	14,800 ± 100	1000[b]	16,207–16,656	Ostracods
KIA 25684	1680–1700	1374–1394	16,120 ± 90	1450[c]	17,135–18,217	Ostracods
KIA 25685	1815–1835	1509–1529	17,090 ± 110	1450[c]	18,591–19,348	Ostracods
KIA 25686	2535–2555	2095–2115	19,390 ± 110	1450[c]	20,772–21,879	Ostracods
Y-2/Cape Riva tephra	2652	2192	18,310 ± 380[d]	–	21,270–22,290[e]	Pichler and Friedrich, 1976, Erikson et al., 1990
KIA 25687	2800–2820	2295–2315	20,240 ± 130	1450[c]	21,744–22,916	Ostracods
KIA 25754	3025–3045	2497–2517	21,030 ± 160	1450[c]	22,720–23,863	Gastropod
KIA 25688	3025–3045	2497–2517	21,460 ± 140	1450[c]	23,353–24,527	Ostracods
KIA 25678	3310–3332	2726–2748	22,340 ± 190	1450[c]	24,521–25,595	Ostracods

[a] Calibrated date range calculated by CALIB. 5.0.1 (Stuiver et al., 2005) using the IntCal04 curve (Reimer et al., 2004).
[b] Reservoir correction was inferred by comparison to other Black Sea records and GISP2 record, therefore no error estimation is given.
[c] Estimated reservoir correction. The error estimation calculated according to the formula $(\sigma^2_{lacustrine} + \sigma^2_{atmospheric})^{1/2}$ falls into range 390–425 ^{14}C yr and gives an average value of 400 ^{14}C yr.
[d] Mean and standard deviation of original dating series.
[e] Mean and standard deviation of calibrated ranges of original dating series.

https://doi.org/10.1016/j.yqres.2008.12.004 Published online by Cambridge University Press

published records from the western Black Sea (Kwiecien et al., 2008). The correlation was performed visually with the program ICC (by Norbert Nowaczyk, GFZ Potsdam) using XRF Ca-intensity and $CaCO_3$ concentration records. For consistency, Black Sea records from other publications presented herein are tuned to the MD04-2788/2760 time scale.

Results

Profiling measurements and $CaCO_3$ content

Very high sedimentation rates at the study site result in low-amplitude changes in the composition of the terrigenous fraction. The

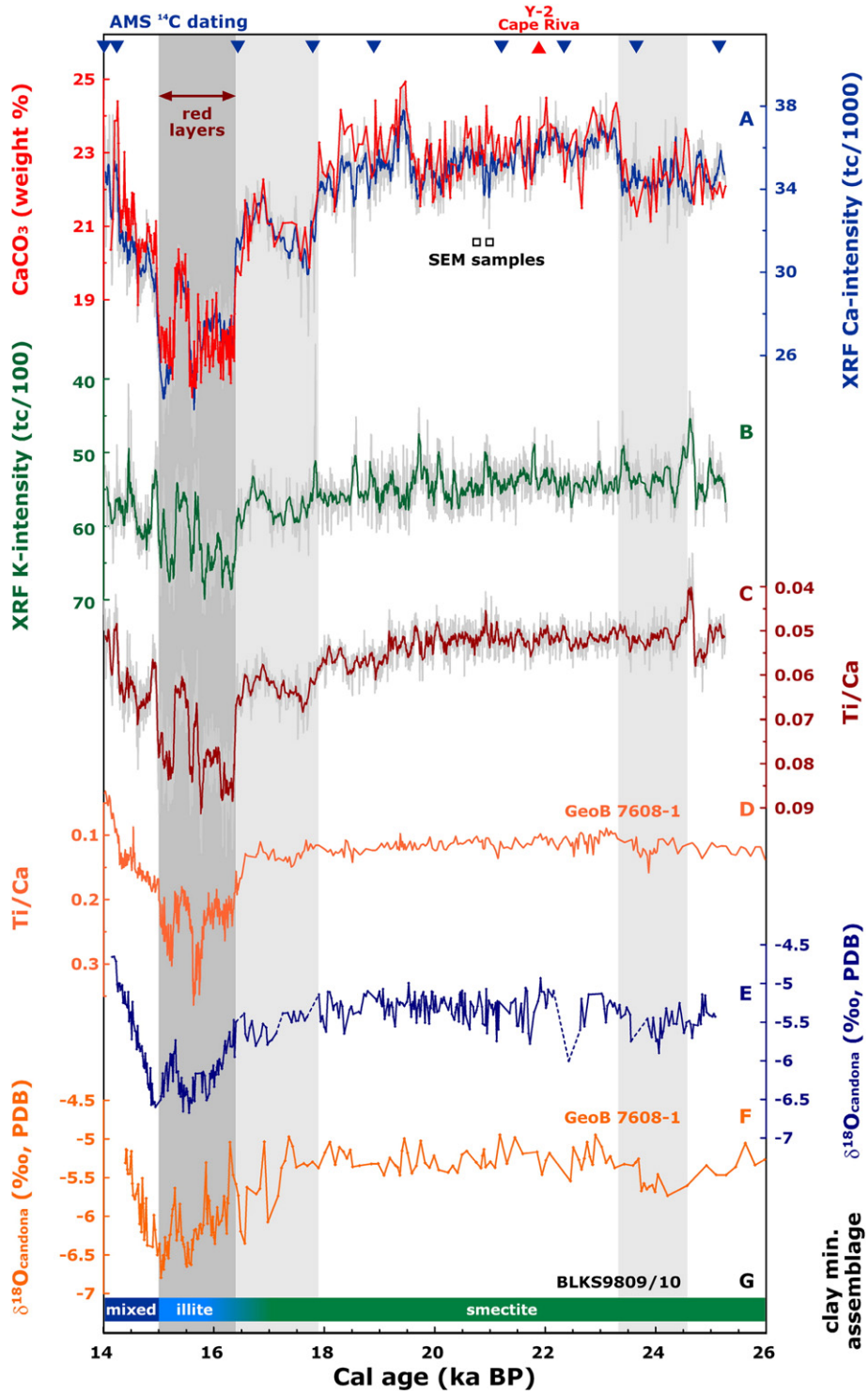

Figure 3. Paleoclimate records from different cores in the Black Sea. The chronology of core MD04-2788/2760 is based on reservoir-corrected calibrated ^{14}C ages (Kwiecien et al., 2008). (A–C, E) data from the MD04-2788/2760; in case of XRF data thin gray lines represent original data and thick color lines represent a 7-point moving average. (A) Corrected XRF Ca-intensity record (tc/1000) in blue, $CaCO_3$ (wt.%) in red. (B) XRF K-intensity record (tc/100). (C) XRF Ti/Ca ratio. (D) XRF Ti/Ca ratio from the core GeoB 7608-1 (Bahr et al., 2005). (E) $\delta^{18}O$ measured on ostracods. (F) $\delta^{18}O$ measured on ostracods from the core GeoB 7608-1 (Bahr et al., 2006). (G) Clay mineral assemblage from the cores BLKS9809/10 (Major et al., 2002). Light gray bars indicate periods of reduced carbonate supply, dark gray bar indicates period of reduced carbonate supply related to red layers.

https://doi.org/10.1016/j.yqres.2008.12.004 Published online by Cambridge University Press

high-resolution XRF Ca-intensity record is reproduced by bulk $CaCO_3$ measurements (Fig. 3A), suggesting that Ca primarily represents carbonates. We ascribed the apparent difference between the two records at 19.5–18 cal ka BP to the intense water condensation during the XRF profiling (Tjallingii et al., 2007) and corrected the XRF data in this interval using a linear relationship between XRF Ca-intensity and $CaCO_3$ content. The $CaCO_3$ content ranges from 25 to 16.3 wt.%. Both $CaCO_3$ content and XRF Ca-intensity show 3 minima at 24.5–23.5 cal ka BP, 18–17 cal ka BP, and 16.4–15 cal ka BP. The last and most pronounced carbonate minimum, at 16.4–15 cal ka BP, is coeval to the period of the 'red layers' deposition. After 15 cal ka BP the carbonate content gradually increases and at 14 cal ka BP reaches the values observed for the period between 23 and 18 cal ka BP.

Fe, Ti and K intensities are commonly linked to siliciclastic components. Ratios of Fe, Ti or K to Ca can be used to represent variations in the relative proportion of siliciclastic and biogenic carbonate sedimentation. However, carbonates from the glacial sediments of the Black Sea are known to be dominantly detrital (Müller and Stoffers, 1974). Scanning Electron Microscope (SEM) analysis and sieving proved absence of authigenic carbonates throughout the glacial and suggested that a dominant portion of the carbonate fraction is of detrital origin and was transported to the study site in the clay/silt fraction (Fig. 4), together with siliciclastics (a negligible amount of non-detrital carbonate fraction consists of gastropod and ostracod shells).

We have chosen the K intensity and Ti/Ca ratio to trace changes in the composition of the terrigenous fraction. A significant part of K must come from K-rich clay minerals (e.g., illite) and K-feldspars which are characteristic for the northern sediment provenance of the Black Sea (Müller and Stoffers, 1974). K-intensity (Fig. 3B) and Ti/Ca ratio (Fig. 3C) stay on moderately stable level throughout the glacial and both abruptly increase after 16.4 cal ka BP. The period of increased K-intensity and Ti/Ca ratio correlates with the occurrence of red layers. Comparable enrichment in Ti and K during the red layers deposition can be observed in the cores from the northern transect (Bahr et al., 2005). The Ti/Ca ratio from core MD04-2788/2760 shows very similar pattern to the GeoB 7608-1 record from the northwestern Black Sea (Bahr et al., 2005) (Fig. 3D). However, Ti/Ca values are generally lower (~3-fold decrease) in the north. The change in the elemental composition in the MD04-2788/2760 and GeoB 7608-1 starting at 16.4 cal ka BP coincides with the change in the clay mineral assemblage composition recorded in the northwestern Black Sea (Major et al., 2002) (Fig. 3G).

Stable isotopes

The isotopic composition of ostracod valves reflects the isotopic composition and temperature of the water mass at the time of valve calcification and therefore provides important information on the hydrology of the basin. However, it is known that ostracods do not calcify in equilibrium with the ambient water but show, within related genera, constant temperature-independent offsets. The vital offset determined for the genus *Candona* should be near to +2.2‰ (von Grafenstein et al., 1999). $\delta^{18}O$ measurements from cores MD04-2788/2760 (Fig. 3E) reveal a relatively stable level during the glacial period. Between 25 and 16.4 cal ka BP the $\delta^{18}O$ values oscillate around −5.3‰. A gradual but significant depletion of ~1‰ is observed during the deposition of the red layers between 16.4 and 15 cal ka BP. Within the thousand years after the deposition of the red layers, $\delta^{18}O$ values rise back to their glacial level. Our results parallel the NW Black Sea record (core GeoB 7608-1) very well, measured on the same genus *Candona* spp. published by Bahr et al. (2006) (Fig. 3F). Only the two negative $\delta^{18}O$ excursions directly before the onset of the red layer are more pronounced in GeoB 7608-1 than in MD04-2788/2760.

Discussion

Past rainfall variability

During the glacial period, sedimentation in the isolated Black Sea was dominated by fluvial input. Based on the very proximal core location to the river mouth, we assume that the major portion of the sediment was delivered to the MD04-2788/2760 site by the Sakarya River. Comparable XRF Ca-intensity patterns (Kwiecien et al., 2008) together with an enrichment in smectite (Major et al., 2002) (Fig. 3G) observed in the northern cores (collected from the continental slope beyond the mouth of the Danube River) suggest that prior to 16.4 cal ka BP, sediments from the southern provenance were penetrating farther northward into the Black Sea.

Fluvial supply of terrigenous material is dependent on two factors: precipitation and the vegetation in the catchment area. Palynological investigations from Anatolia (Fontugne et al., 1999 and reference therein) suggest sparse vegetation cover and domination of steppe taxa throughout our study period (14–26 cal ka BP). As available evidence point to reduced variability of the glacial vegetation (mostly steppe-like accommodated to arid conditions), we assume that modifications in vegetation cover during that time were not sufficient enough to affect the continental runoff on a centennial time scale. Consequently, changes in the terrigenous supply can be expressed as a function of past rainfall variability. Potential complications, for example through increased river runoff due to summer melting of mountain glaciers are unlikely, as there is no compelling evidence for the presence of glaciers during the late Pleistocene in western Anatolia (Ciner, 2004).

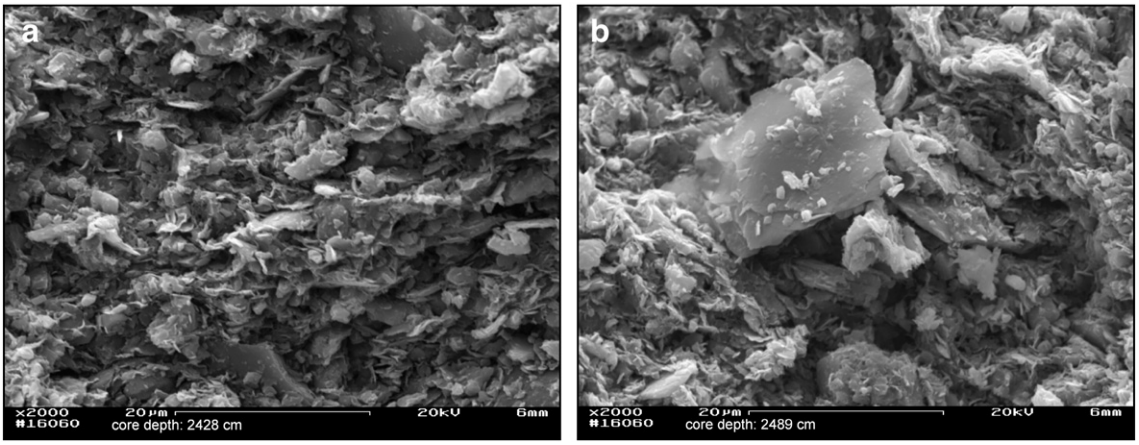

Figure 4. Scanning electron macrographs of sediment samples from selected intervals of the glacial section of core MD04-2760. Original sample depth, magnification and scale are indicated on the picture. The age of the sampled intervals is also shown on the Fig. 3. The sediment is composed mostly of mud with sporadic bigger mica or feldspar crystals. Note a mica crystal in the center of picture b.

https://doi.org/10.1016/j.yqres.2008.12.004 Published online by Cambridge University Press

Today, the sediment load of the Sakarya River follows the regional seasonal precipitation pattern with the highest rainfall during the winter/spring months (Fig. 2b). The rainfall variability in western Anatolia will particularly affect the carbonate-bearing lower course of the Sakarya River and will be expressed as relative changes in the carbonate content of the sediment. A very good agreement between the high-resolution XRF Ca-intensity and $CaCO_3$ concentration in our record (Fig. 3A) proves that Ca is bound in the calcium carbonates. We then assume that the $CaCO_3$ content in our record represent the contribution of the more rainfall-sensitive coastal mountain area and can thus be considered as an indicator for terrigenous supply from this region. With the modern relation of sediment load to regional rainfall pattern (Algan et al., 1999) as an analog, the $CaCO_3$ content in glacial times can be used as proxy for relative changes in the regional precipitation in the western Anatolia.

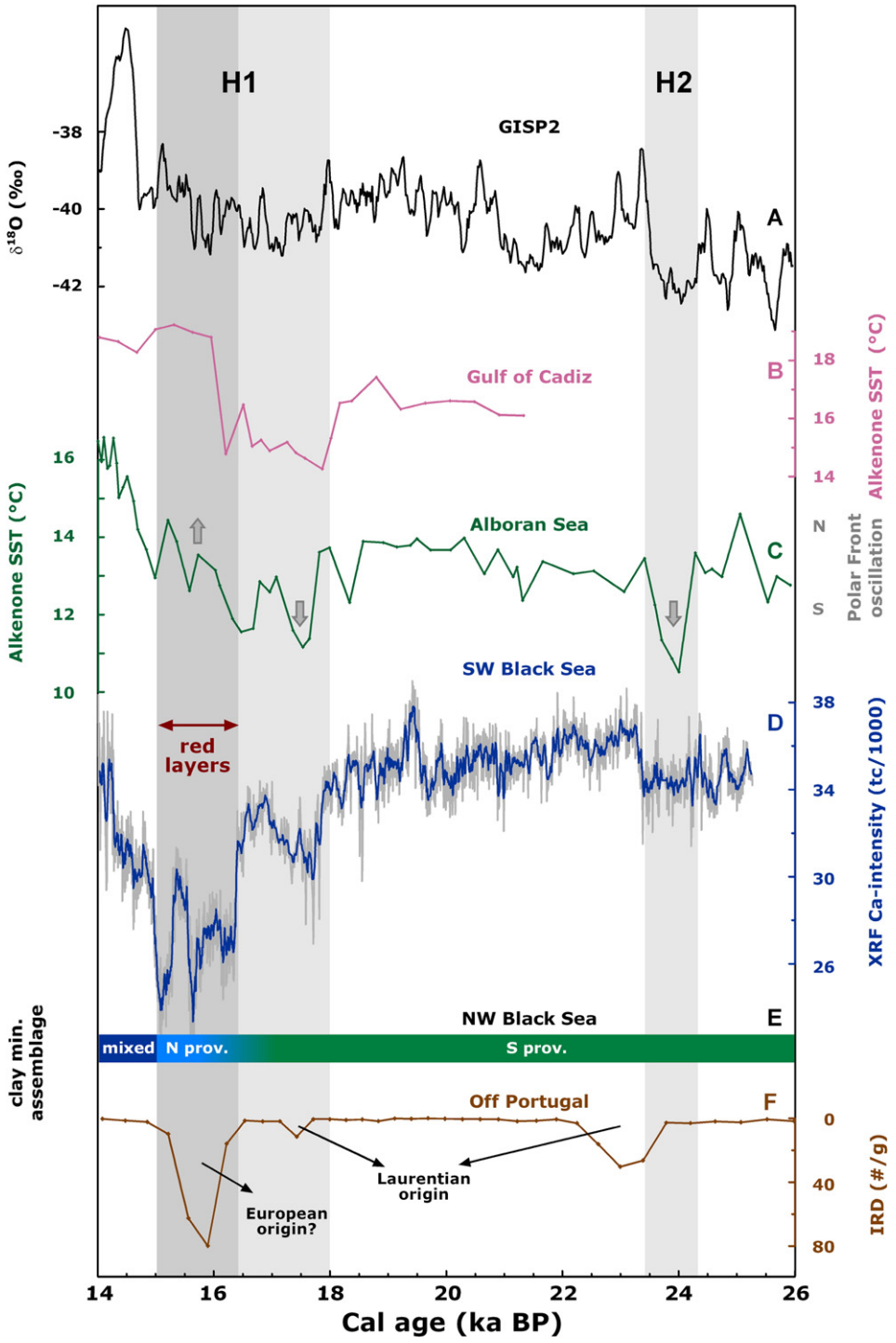

Figure 5. Juxtaposition of different climatic records covering LGM in the Mediterranean region (4B–4F); GISP2 stratigraphy given for comparison (4A). The gray arrows indicate direction of the latitudinal displacements of the polar fronts inferred from western Mediterranean SST records (based on Cacho et al., 2001, and Rohling et al., 1998). XRF Ca-intensity record from MD04-2788/2760 was corrected using the linear relation to $CaCO_3$ weight percentage. (A) GISP2 (Grootes et al., 1993); (B) M39-008 (Cacho et al., 2000); (C) MD95-2043 (Cacho et al., 2000); (E) BLKS9809/10 (Major et al., 2002); (F) SU8118 (Bard et al., 2000). Timing of H1 and H2 (after Bard et al., 2000) is indicated by the gray bars. For H1, light gray bar marks cold phase and the dark gray bar marks purported warming phase (see text). Except for GISP2, the locations of all sites are shown in Fig. 1.

https://doi.org/10.1016/j.yqres.2008.12.004 Published online by Cambridge University Press

Link between the North Atlantic Heinrich events and Black Sea precipitation

Today the southwestern coast of the Black Sea is influenced mainly by Mediterranean moisture sources and receives most of the rainfall during the winter season (Türkes and Erlat, 2005). The intensity of cyclones supplying moisture towards the east is strongly related to the Mediterranean SSTs.

In general, relative precipitation changes in our glacial record (Fig. 5D) coincide well with changes in the western Mediterranean SST records (Cacho et al., 2001) (Figs. 5B, C), indicating drier conditions during lowered SSTs and consequently suggesting that during the glacial, the regional rainfall variability was, similar like today, controlled by the Mediterranean cyclonic disturbances (low-pressure cells, Fig. 1; Wigley and Farmer, 1982). SST minima in the Mediterranean (Figs. 5B, C) (Cacho et al., 2001) were related to Heinrich events H1 and H2 (Grootes et al., 1993) (Fig. 5A; timing of the H1 and H2 after Bard et al., 2000). During the glacial period, extended continental ice sheets and sea ice resulted in a southward expansion of the polar zone, which strengthened the westerly jet, displaced it towards the equator, and increased the temperature gradient between mid- and low-latitudes (Chapman and Maslin, 1999). A southward-shifted jet stream would have led to relatively wet conditions in southern Europe and the Mediterranean, leaving the central and northern Europe relatively drier. Both polar water and polar air masses reached a maximum southward expansion during Heinrich events (Rohling et al., 1998). This southward migration of the North Atlantic polar front and atmospheric Polar Front was related to the calving of sea ice and the waxing of continental ice sheets, respectively. SST minima recorded during Heinrich events in the western Mediterranean (Figs. 5B, C) were related either to the entrance of cold water from the Atlantic Ocean (Cacho et al., 1999, 2001; Sierro et al., 2005) and/or to the atmospheric conditions over the Mediterranean Sea, such as the intensified flow of dry and cold winds (Rohling et al., 1998; Cacho et al., 2000, 2006) (Fig. 5C).

Although the temperature gradient between mid- and low latitudes stayed high and the westerly jet stayed south, cooler Mediterranean SSTs occurring during HEs would have decreased the atmosphere–sea surface thermal gradient, resulting in a weakening of the Mediterranean low-pressure systems. Subsequent, less frequent and less intense storms would have led to significantly reduced precipitation in the eastern Mediterranean/Black Sea region. Additionally, decreased air temperatures would have reduced the water vapor capacity, thus hindering an eastward moisture transport. A similar scenario has already been proposed to link arid episodes in the eastern Mediterranean with the Heinrich events (Bartov et al., 2003). Enhanced aridity during Heinrich events is documented by pollen records in the western Mediterranean (Combourieu Nebout et al., 2002; Sánchez Goñi et al., 2002) and by low lake levels in the eastern Mediterranean, such as that of Lake Lisan (Bartov et al., 2003) and other Turkish lakes in the Konya Plain (Fontugne et al., 1999, and references therein). Thus, the precipitation decrease interpreted from our record during H2 can be directly linked to the cooling of the Mediterranean.

Mixed nature of H1 and switch in the dominant sediment source

The signature of the Black Sea records during H1 (*sensu* Bard et al., 2000) is more complex. The initial decrease in carbonate concentration at ~18 cal ka BP, indicating a decrease in northeast Anatolian precipitation, was followed by a more pronounced decrease in carbonate content at 16.4 cal ka BP. The latter coincides with prominent changes in the composition of the terrigenous fraction and with a series of meltwater pulses reflected by the $\delta^{18}O$ signal (Figs. 3E, F). Unlike the two previous carbonate concentration minima, this period starting at 16.4 cal ka BP is characterized by high sedimentation rates (not shown) and corresponds to a rise of Mediterranean SSTs (Figs. 5B, C).

The abrupt decrease in the $CaCO_3$ content at 16.4 cal ka BP (Fig. 3A) accompanied by an increase in XRF K-intensity and the Ti/Ca ratio (Figs. 3B, C) could imply either a drastically reduced carbonate supply (reduced rainfall) and/or an intensification of a previously less active source.

In the north of the Black Sea, the concomitant increase of the Ti/Ca ratio during the red layers interval (Fig. 3D) was linked to the enrichment of fine clay material brought by meltwater inflow coming from the north (Bahr et al., 2005). This interpretation was further strengthened by $\delta^{18}O$ data (Bahr et al., 2006), showing temporary isotopic depletion subsequent to each of the meltwater pulses (Fig. 3F) represented by Ti/Ca peaks (Fig. 3D). Our Ti/Ca record displays very similar fluctuations but of somewhat lower magnitude, which could be explained by the northwards-decreasing amount of detrital carbonates (Müller and Stoffers, 1974). Changes in our Ti/Ca ratio and XRF K-intensity correlate well with changes in the dominant sediment source at 16.4 cal ka BP, recorded as a shift in the clay mineral assemblage data (Major et al., 2002) (Fig. 3G). Therefore, we interpret the Ti/Ca and K variability during H1 in terms of changes in the relative contribution of a southern (Sakarya River) versus a northern sediment source.

The modification in the freshwater sources after 16.4 cal ka BP is recorded by the $\delta^{18}O$ data. The congruent isotope pattern from north and south of the Black Sea (Figs. 3E, F) indicates that the hydrological response to the meltwater injection was uniform on a basin scale, and further suggests that the water column was well mixed at the time of the inflow. Moreover, the very good agreement between $\delta^{18}O$ records of MD04-2788/2760 and GeoB 7608-1 provides an independent proof for the accuracy of the Ca-signal-tuned chronology.

According to Konikov et al. (2007), the level of the Black Sea was gradually rising since the LGM. Sea level rise can significantly influence sedimentation processes in big basins, with exposing/drowning shelf areas functioning as traps for coarser sediments (e.g., Ehrmann et al., 2007). During the red layers' deposition, changes in the grain size (Bahr et al. 2005) and in sedimentation rates (not shown) were accompanied by significant compositional changes of the sediment. Therefore we suspect that even if the lake level slightly rose during this meltwater inflow, it probably played only a minor role for the observed depositional changes and the contribution from an additional source was more important.

Several factors consistent with reconstructions of central and north European climate can explain the suppression of sediment supply from the northern Black Sea provenance until ~16 cal ka BP. During the LGM, cold and arid conditions prevailed in the northern and western drainage areas of the Black Sea (Florineth and Schluchter, 2000; Atanassova, 2005) and soils in the northern catchment remained partly frozen (Renssen and Bogaart, 2003). The retraction of Scandinavian ice sheets (Rinterknecht et al., 2006) and Alpine glaciers (Florineth and Schluchter, 2000) during the LGM suggest that the mid-latitudes may have suffered from moisture starvation at that time. Lake status data from northwestern Europe indicate similarly dry conditions (Harrison et al., 1996). Low precipitation would result in reduced fluvial runoff of the northern (Don, Dniepr, Dniester) and western (Danube) rivers, while permafrost could have inhibited the erosion in the catchment. Dry conditions in northern Europe during the glacial are consistent with the more southerly position of the polar fronts and westerlies, and wetter southern Europe and Mediterranean region.

The intensification of the northern sediment/freshwater source after 16.4 cal ka BP is contemporary with the onset of deglacial warming in Europe. It roughly corresponds to the time when the Scandinavian ice sheet (SIS) blocked the drainage towards the Baltic Sea (Mangerud et al., 2004; Svendsen et al., 2004). Meltwater from a

https://doi.org/10.1016/j.yqres.2008.12.004 Published online by Cambridge University Press

considerable sector of the SIS was proposed to have flowed into the watershed of the Volga River (Mangerud et al., 2004). Enhanced Volga runoff would cause the Caspian Sea to overflow along the Manych Depression to the Black Sea (Bahr et al., 2005; Mangerud et al., 2004).

The possibility of the late-glacial Black Sea–Caspian Sea connection was challenged by Major et al. (2006), arguing that $^{87}Sr/^{86}Sr$ ratio of the modern Caspian Sea is too low to account for the $^{87}Sr/^{86}Sr$ changes seen in the Black Sea during the deposition of the red layers. Initial investigation of new cores retrieved from the northeastern Black Sea basin south of the Sea of Azov (R/V *Meteor* cruise 72/5, unpublished data) revealed no presence of red layers at the expected depth. This could imply that red layers are confined only to the western Black Sea basin, which would in turn exclude their relation to the potential Caspian outflow. In addition, the rerouting of north European river systems and the direction of the meltwater discharge from the SIS is still a matter of debate. Meltwater could have been directed not only to the south, as initially suggested by Mangerud et al. (2004), but also towards the Baltic Sea, much farther west to the Bay of Biscaye (Menot et al., 2006), or to the Arctic Ocean in the north (Demidov et al., 2006). Notably, in case the SIS advanced into the watersheds of the Volga River (Mangerud et al., 2004), a similar process could have taken place in the watershed of the Dniepr River (Kalicki and Sanko, 1998). Feeding of the Dniepr River by thawing glaciers would usher a meltwater flow directly into the Black Sea without the necessity of the Caspian Sea basin as an intermediary. Alternatively, as first proposed by Major et al. (2002), thawing of the permafrost in the Dniepr River watersheds could have led to increased runoff in the northern drainage area and enhanced sediment transport of fine clay particles.

The qualitative nature of our proxies makes it difficult to state clearly whether the contribution of the southern source had diminished after 16.4 cal ka BP, or if it stayed at the previous level but was counterbalanced by the growing influence of a northern source (Fig. 5E). The sedimentation rate in the MD04-2788/2760 is comparatively high during the red layers' deposition as during most of the LGM, suggesting that the sediments from the southern provenance were diluted rather than replaced by the contribution of the northern source. In this case, precipitation in NW Anatolia should have stayed at a relatively high level over that time. The lowered level of lakes in the Mediterranean region at that time point to enhanced aridity after 16.4 cal ka BP (Bartov et al., 2003; Harrison et al., 1996). However, quantitative reconstructions based on stable oxygen isotopes (Bar-Matthews et al., 1997; Jones et al., 2007) clearly suggest an increase in rainfall amount. This apparent dissonance between lake level and isotope records may arise from a different sensitivity to different components of the water balance. Since the lake level is controlled by precipitation-to-evaporation ratio, the lowering of the lake level after H1 can be explained by the temperature increase leading to higher evaporation and not necessarily by decreased precipitation.

Marine Mediterranean records document a significant reorganization of the oceanic/atmospheric circulation at that time (Cacho et al., 2001; Sierro et al., 2005) including regional warming. The sharp warming phase in the Gulf of Cadiz (Fig. 5B) probably corresponds to a rapid northward migration of the North Atlantic polar front (Cacho et al., 2001). A northward-retreating polar fronts would have had an effect opposite to the glacial situation: decreased temperature gradients between mid- and low latitudes, a weakened westerly jet, and a shift of the precipitation belt back north towards the continent. A readvance of woodlands in central Europe (Atanassova, 2005) and the establishment of lowland forests in southeastern Alps (Vescovi et al., 2007) after ~16 cal ka BP point to an increase in rainfall in the north and west of the Black Sea.

Taken together, within the time frame of H1 (*sensu* Bard et al., 2000) only the initial decrease in precipitation amount at 18–17 cal ka BP inferred from the MD04-2788/2760 record corresponds to the North Atlantic cooling event. The following 'apparent' precipitation minima, caused by the dilution of southern provenance sediment by the enhanced contribution of the northern provenance starting at 16.4 cal ka BP, is contemporary to an increase of the Mediterranean SSTs and can be related to the northward retreat of the polar front (Fig. 5C). Sánchez Goñi et al. (2000) described a three-phase pattern of Heinrich events in the mid-latitudes of the North Atlantic region, first with a cold and humid phase, then a cold and dry middle phase related to massive iceberg discharge from the Laurentide ice sheet, and finally a mild and humid third phase linked to the disintegration of the European ice sheets. Bard et al. (2000) also showed that in the Subtropical Northeast Atlantic, ice-rafted debris (IRD) has a different composition during the first phase of H1 than during the last phase (Fig. 5F), suggesting multiple origins of the ice surges (including the Fennoscandian ice sheet). The intensification of the northern sediment/freshwater source observed in our record after 16.4 cal ka BP fits well to the scenario of European ice sheets melting and the mitigation of the central and north European climate.

Conclusions

During the last glacial, rainfall in western Anatolia was responding to changes in Mediterranean SSTs. Periods of reduced precipitation recorded in the Black Sea sediments correlate to Heinrich events H1 and H2, and support the idea of a strong link between the mid- and high-latitudes. Until ~16.4 cal ka BP, precipitation associated with the Mediterranean cyclonic disturbances was controlling the supply of terrigenous material in the southern drainage of the western Black Sea basin. Intensification of northern sediment/freshwater sources at ~16.4 cal ka BP coincides with major postglacial reorganizations of atmospheric and/or oceanic circulation patterns. This observation is coherent with other climatic records pointing to a shift in the European moisture source distribution. Our indirect record of northwest Anatolian precipitation and changes in relative contribution of southern and northern sediment sources agrees well with SST records from the western Mediterranean (Cacho et al., 2001) and lake level records from the eastern Mediterranean (Fontugne et al., 1999; Bartov et al., 2003) and north Eurasia (Harrison et al., 1996). The intensification of a northern sediment source paralleled the northward retreat of the polar fronts after ~16.4 cal ka BP which accounted for warming in the Mediterranean region and more humid conditions in central and northern Europe.

Acknowledgments

This research was sponsored by Comer Science and Education Foundation (CS&EF). We thank IPEV for logistic support during the ASSEMBLAGE I cruise (RV *Marion Dufresne*). We also thank M. Segl, University of Bremen, and her team for performing the stable isotope analysis, U. Röhl, University of Bremen, for support in XRF measurements, A. Hendrich, GFZ Potsdam, for graphic assistance with the topographic map and a Spectral Electron Microscope team; H. Kemnitz and J. Herwig, GFZ Potsdam, for introduction to the SEM facility. We appreciate the help of Gerhard Schmiedl and an anonymous reviewer whose comments improved our manuscript.

References

Algan, O., Gazioglu, C., Cagatay, M.N., Yücel, Z.Y., Gonencgil, B., 1999. Sediment and water influxes into the Black Sea by Anatolian rivers. Z. Geomorph. N. F. 43, 61–67.

Allen, J.R.M., Brandt, U., Brauer, A., Hubberten, H.-W., Huntley, B., Keller, J., Kraml, M., Mackensen, A., Mingram, J., Negendank, J.F.W., Nowaczyk, N.R., Oberhansli, H., Watts, W.A., Wulf, S., Zolitschka, B., 1999. Rapid environmental changes in southern Europe during the last glacial period. Nature 400, 740–743.

Atanassova, J., 2005. Palaeoecological setting of the western Black Sea area during the last 15000 years. The Holocene 15 (4), 576–584.

Bahr, A., Lamy, F., Arz, H., Kuhlmann, H., Wefer, G., 2005. Late glacial to Holocene climate and sedimentation history in the NW Black Sea. Mar. Geol. 214, 309–322.

Bahr, A., Arz, H.W., Lamy, F., Wefer, G., 2006. Late glacial to Holocene paleoenvironmental evolution of the Black Sea, reconstructed with stable oxygen isotope records obtained on ostracod shells. Earth Planet. Sci. Lett. 241, 863–875.

https://doi.org/10.1016/j.yqres.2008.12.004 Published online by Cambridge University Press

Bahr, A., Arz, H.W., Lamy, F., Major, C., Kwiecien, O., Wefer, G., 2008. Abrupt changes of temperature and water chemistry in the late Pleistocene and early Holocene Black Sea. G-cubed 9, doi:10.1029/2007GC001683.
Bar-Matthews, M., Ayalon, A., Kaufman, A., 1997. Late Quaternary paleoclimate in the Eastern Mediterranean Region from stable isotope analysis of speleothems at Soreq Cave, Israel. Quat. Res. 47, 155–168.
Bard, E., Rostek, F., Turon, J.-L., Gendreau, S., 2000. Hydrological impact of Heinrich events in the subtropical Northeast Atlantic. Science 289, 1321–1324.
Bartov, Y., Goldstein, S.L., Stein, M., Enzel, Y., 2003. Catastrophic arid episodes in the Eastern Mediterranean linked with the North Atlantic Heinrich events. Geology 31, 439–442.
Bond, G., Broecker, W.S., Johnsen, S.J., McManus, J., Labeyrie, L., Jouzel, J., Bonani, G., 1993. Correlations between climate records from North Atlantic sediments and Greenland ice. Nature 365, 143–147.
Cacho, I., Grimalt, J.O., Pelejero, C., Canals, M., Sierro, F.J., Flores, J.A., Shackleton, N., 1999. Daansgard-Oeschger and Heinrich event imprints in Alboran Sea paleotemperatures. Paleoceanography 14, 689–705.
Cacho, I., Grimalt, J.O., Sierro, F.J., Shackleton, N., Canals, M., 2000. Evidence for enhanced Mediterranean thermohaline circulation during rapid climatic coolings. Earth Planet. Sci. Lett. 183, 417–429.
Cacho, I., Grimalt, J.O., Canals, M., Sbaffi, L., Shackleton, N.J., Schönfeld, J., Zahn, R., 2001. Variability of the western Mediterranean Sea surface temperature during the last 25 000 and its connection the Northern Hemisphere climatic changes. Paleoceanography 16, 40–52.
Cacho, I., Shackleton, N., Elderfield, H., Sierro, F.J., Grimalt, J.O., 2006. Glacial rapid variability in deep-water temperature and d18O from the Western Mediterranean Sea. Quat. Sci. Rev. 25, 3294–3311.
Chapman, M.R., Maslin, M.A., 1999. Low-latitude forcing of meridional temperature and salinity gradients in the subpolar North Atlantic and the growth of glacial ice sheets. Geology 27, 875–878.
Ciner, A., 2004. Turkish glaciers and glacial deposits. In: Ehlers, J., Gibbard, P.L. (Eds.), Quaternary Glaciations; Extentand Chronology, Part I: Europe. Elsevier Publishers, Amsterdam, pp. 419–429.
Combourieu Nebout, N., Turon, J.L., Zahn, R., Capotondi, L., Londeix, L., Pahnke, K., 2002. Enhanced aridity and atmospheric high-pressure stability over the western Mediterranean during the North Atlantic cold events of the past 50 ky. Geology 30, 863–866.
Demidov, I.N., Houmark-Nielsen, M., Kjaer, K.H., Larsen, E., 2006. The last Scandinavian ice sheet in northwestern Russia: ice flow patterns and decay dynamics. Boreas 35, 425–443.
Ehrmann, W., Schmiedl, G., Hamann, Y., Kuhnt, T., Hemleben, C., Siebel, W., 2007. Clay minerals in late glacial and Holocene sediments of the northern and southern Aegean Sea. Palaeogeogr., Palaeoclimatol., Palaeoecol. 249, 36–57.
EIE, State General Directory of Electrical Research Works, 1993. Sediment data and sediment transport amount for surface waters in Turkey. EIE, Ankara, Turkey.
Florineth, D., Schluchter, C., 2000. Alpine evidence for atmospheric circulation patterns in Europe during the last glacial maximum. Quat. Res. 54, 295–308.
Fontugne, M., Kuzucuoglu, C., Karabiyikoglu, M., Hatte, C., Pastre, J.-F., 1999. From Pleniglacial to Holocene: a 14C chronostratigraphy of environmental changes in the Konya Plain, Turkey. Quat. Sci. Rev. 18, 573–591.
Geological Research Department of the General Directorate of Mineral Research and Exploration, 2002, Geological Map of Turkey.
Grootes, P., Stuvier, M., White, J.W.C., Johnsen, S.J., Jouzel, J., 1993. Comparison of oxygen isotope records from the GISP2 and GRIP Greeenland ice cores. Nature 366, 552–554.
Harrison, S.P., Yu, G., Tarasov, P.E., 1996. Late Quaternary lake-level record from Northern Eurasia. Quat. Res. 45, 138–159.
Jansen, J.H.F., Van der Gaast, S.J., Koster, B., Vaars, A.J., 1998. CORTEX, a shipboard XRF-scanner for element analyses in split sediment cores. Mar. Geol. 151, 143–153.
Jones, M.D., Roberts, C.N., Leng, M.J., 2007. Quantifying climatic change through the last glacial-interglacial transition based on lake isotope palaeohydrology from central Turkey. Quat. Res. 67, 463–473.
Kalicki, T., Sanko, A.F., 1998. Palaeohydrological changes in the Upper Dneper Valley, Belarus, during the last 20,000 years. In: Benito, G., et al. (Ed.), Palaeohydrology and Environmental Change. Wiley, Chichester, England, pp. 125–135.
Konikov, E., Likhodedova, O., Pedan, G., 2007. Paleogeographic reconstruction of sea-level change and coastline migration on the northwestern Black Sea shelf over the past 18 kyr. Quat. Int. 167–168, 49–60.
Kostopoulou, E., Jones, P.D., 2007. Comprehensive analysis of the climate variability in the eastern Mediterranean. Part II: relationships between atmospheric circulation patterns and surface climatic elements. Int. J. Climatol. 27, 1351–1371.
Kroonenberg, S.B., Rusakov, G.V., Svitoch, A.A., 1997. The wandering of the Volga delta: a response to rapid Caspian sea-level change. Sediment. Geol. 107, 189–209.
Kwiecien, O., Arz, H.W., Lamy, F., Wulf, S., Bahr, A., Röhl, U., Haug, G.H., 2008. Estimated reservoir ages of the Black Sea since the last glacial. Radiocarbon 50, 99–118.
Lamy, F., Arz, H.W., Bond, G., Bahr, A., Patzold, J., 2006. Multicentennial-scale hydrological changes in the Black Sea and northern Red Sea during the Holocene and the Arctic/North Atlantic Oscillation. Paleoceanography 21, doi:10.1029/2005PA001184.
Major, C., Ryan, W., Lericolais, G., Hajdas, I., 2002. Constraints on Black Sea outflow to the Sea of Marmara during the last glacial-interglacial transition. Mar. Geol. 190, 19–34.
Major, C.O., Goldstein, S.L., Ryan, W.B.F., Lericolais, G., Piotrowski, A.M., Hajdas, I., 2006. The co-evolution of Black Sea level and composition through the last deglaciation and its paleoclimatic significance. Quat. Sci. Rev. 25, 2031–2047.
Mangerud, J., Jakobsson, M., Alexanderson, H., Astakhov, V., Clarke, G.K.C., Henriksen, M., Hjort, C., Krinner, G., Lunkka, J.-P., Moller, P., 2004. Ice-dammed lakes and rerouting of the drainage of northern Eurasia during the last glaciation. Quat. Sci. Rev. 23, 1313–1332.
Menot, G., Bard, E., Rostek, F., Weijers, J.W.H., Hopmans, E.C., Schouten, S., Damste, J.S.S., 2006. Early reactivation of European rivers during the last deglaciation. Science 313, 1623–1625.
Mudie, P.J., Rochon, A., Aksu, A.E., Gillespie, H., 2002. Dinoflagellate cysts, freshwater algae and fungal spores as salinity indicators in Late Quaternary cores from Marmara and Black seas. Mar. Geol. 190, 203–231.
Mudie, P.J., Marret, F., Aksu, A.E., Hiscott, R.N., Gillespie, H., 2007. Palynological evidence for climatic change, anthropogenic activity and outflow of Black Sea water during the late Pleistocene and Holocene: centennial- to decadal-scale records from the Black and Marmara Seas. Quat. Int. 167–168, 73–90.
Müller, G., Stoffers, P., 1974. Mineralogy and petrology of the Black Sea basin sediments. In: Degens, E.T., Ross, D.A. (Eds.), The Black Sea: Geology, Chemistry, and Biology. AAPG, Tulsa, OK, pp. 200–248.
Prasad, S., Vos, H., Negendank, J.F.W., Waldmann, N., Goldstein, S.L., Stein, M., 2004. Evidence from Lake Lisan of solar influence on decadal- to centennial-scale climate variability during marine oxygen isotope stage 2. Geology 32, 581–584.
Prentice, I.C., Guiot, J., Harrison, S.P., 1992. Mediterranean vegetation, lake levels and paleoclimate at the last glacial maximum. Nature 360, 658–660.
Renssen, H., Bogaart, P., 2003. Atmospheric variability over the ~14.7 kyr BP stadial-interstadial transition in the North Atlantic region as simulated by an AGCM. Clim. Dyn. 20, 301–313.
Reimer, P.J., Baillie, M.G.L., Bard, E., Bayliss, A., Beck, J.W., Bertrand, C.J.H., Blackwell, P.G., Buck, C.E., Burr, G.S., Cutler, K.B., Damon, P.E., Edwards, R.L., Fairbanks, R.G., Friedrich, M., Guilderson, T.P., Hogg, A.G., Hughen, K.A., Kromer, B., McCormac, G., Manning, S., Ramsey, C.B., Reimer, R.W., Remmele, S., Southon, J.R., Stuiver, M., Talamo, S., Taylor, F.W., van der Plicht, J., Weyhenmeyer, C.E., 2004. IntCal04 terrestrial radiocarbon age calibration, 0–26 cal kyr BP. Radiocarbon 43, 1029–1085.
Rinterknecht, V.R., Clark, P.U., Raisbeck, G.M., Yiou, F., Bitinas, A., Brook, E.J., Marks, L., Zelcs, V., Lunkka, J.-P., Pavlovskaya, I.E., Piotrowski, J.A., Raukas, A., 2006. The last deglaciation of the Southeastern sector of the Scandinavian ice sheet. Science 311, 1449–1452.
Rohling, E.J., Hayes, A., Kroon, D., De Rijk, S., Zachariasse, W.J., Eisma, D., 1998. Abrupt cold spells in the NW Mediterranean. Paleoceanography 13, 316–322.
Ryan, W., Major, C., Lericolais, G., Goldstein, S.L., 2003. Catastrophic flooding of the Black Sea. Ann. Rev. Earth Planet. Sci. 31, 525–554.
Sánchez Goñi, M.F., Turon, J.-L., Eynaud, F., Gendreau, S., 2000. European climatic response to millennial-scale changes in the atmosphere–ocean system during the last glacial period. Quat. Res. 54, 394–403.
Sánchez Goñi, M.F., Cacho, I., Turon, J.L., Guiot, J., Sierro, F.J., Peypouquet, J.P., Grimalt, J.O., Shackleton, N.J., 2002. Synchroneity between marine and terrestrial responses to millennial scale climatic variability during the last glacial period in the Mediterranean region. Clim. Dyn. 19, 95–105.
Schrader, H.J., 1979. Quaternary paleoclimatology of the Black Sea basin. Sediment. Geol. 23, 165–180.
Sierro, F.J., Hodell, D.A., Curtis, H.J., Flores, J.A., Reguera, I., Colmenero-Hidalgo, E., Barcena, M.A., Grimalt, J.O., Cacho, I., Frigola, J., Canals, M., 2005. Impact of iceberg melting on Mediterranean thermohaline circulation during Heinrich events. Paleoceanography 20, doi:10.1029/2004PA001051.
Stuiver, M., Reimer, P.J., and Reimer, R.W., 2005, Calib 5.0. (www pragram and documentation). URL: http://calib.qub.ac.uk/calib/.
Svendsen, J.I., Alexanderson, H., Astakhov, V.I., Demidov, I., Dowdeswell, J.A., Funder, S., Gataullin, V., Henriksen, M., Hjort, C., Houmark-Nielsen, M., 2004. Late Quaternary ice sheet history of northern Eurasia. Quat. Sci. Rev. 23, 1229–1271.
Tjallingii, R., Röhl, U., Kölling, M., Bickert, T., 2007. Influence of the water content on X-ray fluorescence corescanning measurements in soft marine sediments. Geochem. Geophys. Geosystems 8, doi:10.1029/2006GC001393.
Touchan, R., Akkemik, U., Hughes, M.K., Erkan, N., 2007. May–June precipitation reconstruction of southwestern Anatolia, Turkey during the last 900 years from tree rings. Quat. Res. 68, 196–202.
Türkes, M., Erlat, E., 2005. Climatological responses of winter precipitation in Turkey to variability of the North Atlantic Oscillation during the period 1930–2001. Theor. Appl. Climatol. 81, 45–69.
Vescovi, E., Ravazzi, C., Arpenti, E., Finsinger, W., Pini, R., Valsecchi, V., Wick, L., Ammann, B., Tinner, W., 2007. Interactions between climate and vegetation during the Lateglacial period as recorded by lake and mire sediment archives in Northern Italy and Southern Switzerland. Quat. Sci. Rev. 26, 1650–1669.
von Grafenstein, U., Erlernkeuser, H., Trimborn, P., 1999. Oxygen and carbon isotopes in modern fresh-water ostracod valves: assessing vital offsets and autecological effects of interest for palaeoclimate studies. Palaeogeogr., Palaeoclimatol., Palaeoecol. 148, 133–152.
Wigley, T.M.L., Farmer, G., 1982. Climate of the Eastern Mediterranean and the Near East. In: Bintliff, J.L., et al. (Ed.), Paleoclimates, Paleoenvironments and Human Communities in the Eastern Mediterranean Region in Later Prehistory, pp. 3–37.